

# ANALYSIS OF LOW-BOOM CHARACTERISTICS OF SUPERSONIC WAVERIDER

Potsawat Boonjaipetch\*

\*Institute of Fluid Science, Tohoku University, Japan

**Keywords:** *Sonic boom, Supersonic, Low-boom*

## Abstract

*Waverider is a famous design concept for generating high lift-to-drag ratio (L/D) at a high Mach number supersonic flow. Due to its high L/D, the concept is also promising for designing hypersonic vehicle. To apply a waverider concept to design a supersonic commercial aircraft, an ability to mitigate sonic boom strength is needed to be well considered. Therefore, in this article, a parametric study of a supersonic waverider at Mach number 1.5 was done by numerical simulation. A cone-derived waverider was studied before further study on more complex shape. The result of parametric study shows some important traits regarding the design of low-boom supersonic waverider from the cone angle and dihedral angle viewpoint. To enrich our knowledge on a low-boom waverider design, a multi-objective optimization procedure was conducted to visualize a physical trade-off between overpressure, lift coefficient and pitching moment coefficient. Sobol indices-based sensitivity analysis was performed using polynomial chaos expansion technique to investigate the relationship between variables and objectives function. In light of the results, we found that the supersonic waverider shows significant potential to mitigate the sonic boom while simultaneously providing high L/D. Furthermore, the present study shows that it is viable to conduct further research with a more complex method for designing and expand the knowledge on waverider for low-boom supersonic aircraft.*

## 1 Introduction

The primary major issues with the supersonic commercial aircraft design are the sonic boom and aerodynamics performance [1]. To that end, it is of utmost importance to seek a low-boom aircraft shape that is able to attain high aerodynamics performance during the high-speed flight. The concept of hypersonic waverider is a promising candidate due to its remarkable high lift-to-drag ratio (L/D) characteristic by nature. The development of the concept of hypersonic waverider has been started around 1990s [2,3] where the trend in aircraft design has been pursued towards greater speed by the innovation of jet engine. Many researchers have attempted to achieve beyond the limit of supersonic travel (i.e., Mach 1 ~ 3) to hypersonic travel (i.e., Mach 5 ~ 25); one important outcome from this research endeavor is the waverider concept. The waverider is any vehicle that uses its own shock wave to improve its overall performance. Whenever a vehicle travels in the air at Mach 1 or higher, it undeniably produces a shockwave. If the aircraft is modified correctly, it can be properly designed so as to ride this wave to produce higher lift, less drag and greater range which leads to overall improved performance [4]. Whenever there is an attached shock generated at the lower surface, it creates greater pressure in its wake. Furthermore, the shock that lies close to the lower surface of the aircraft results in a large pressure force that increases the lift of the vehicle. This idea is known as compression lift and is the primary benefit of the waverider concept.

It is worth noting that the waverider design is primarily applied for designing a hypersonic

vehicle but never shows up in low-supersonic vehicle design such as commercial supersonic aircraft. The goal of this research is to study the cone derived [4,5] waverider method in supersonic design regime. One aim of this research is primarily to discuss the potential of the waverider design in supersonic flight. This study is divided into three stages, that is, parametric study, multi-objective optimization, and data mining. First, the parametric study aims to find the relationship between design parameters and outputs of interest, that is, aerodynamic forces and sonic boom strength. In this study, three design variables were used to generate the waverider design, where the performance is measured using L/D and the far-field overpressure ( $P_{fop}$ ). To enrich the design knowledge, for the second stage, multi-objective optimization is applied to find the optimal combinations of design variables that describe the shape of low-boom waverider by considering three objectives, that is, high lift ( $C_L$ ), low  $P_{fop}$ , and minimize the absolute number of pitching moment ( $C_M$ ). The optimization procedure was conducted by the Non-Sorting Genetic Algorithm II (NSGA2) method assisted by the ordinary Kriging (OK) surrogate model. To gain more design insight, we performed sensitivity analysis to quantify the contribution of the design variables to the objective functions. Through the aforementioned procedures, we aim to gain an essence of supersonic waverider for more practical implementations of supersonic aircraft.

## 2 Parametric Study

### 2.1 A Waverider Geometry

In order to do a parametric study, a simple cone-derived waverider by Rasmussen [5] is used for the present model. The cone-derived waverider is composed by three main surfaces (see Fig.1), that is, a freestream surface, a base plane and a compression surface. The vehicle shape is crafted from an attached shock through a semi-vertex cone body. The design process begins with defining the prescribed cone angle ( $\delta$ ) at a certain free stream Mach number ( $M_\infty$ ) and specific heat ratio ( $\gamma$ ). By solving equation

(1), it is possible to calculate a certain shock angle ( $\beta$ ) using supersonic flow past a cone method which is derived from Taylor-Maccoll equation.

$$\frac{\beta}{\delta} = \left( \frac{\gamma+1}{2} + \frac{1}{M_\infty^2} \right)^{1/2} \quad (1)$$

To generate a waverider [6,7] shape, all points are generated on the free stream trailing edge, the intersection line between freestream surface, and the base plane.

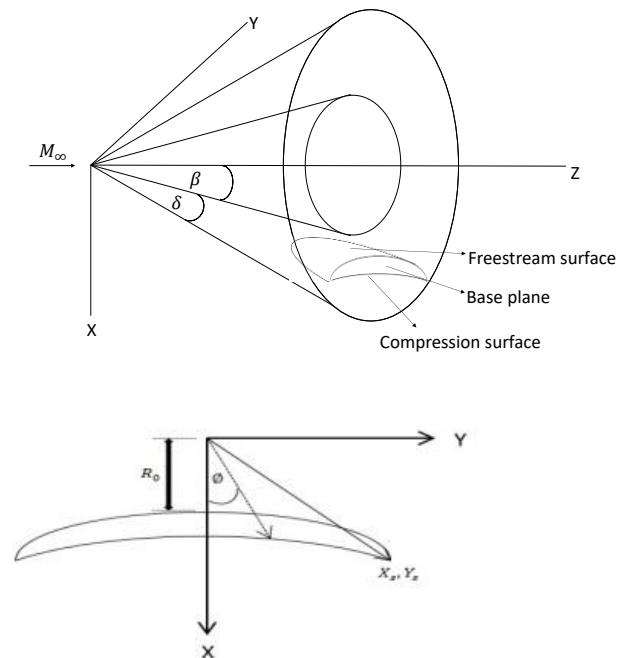


Fig. 1. A cone-derived waverider components and three design variables  $\delta$ ,  $\beta$ , and  $R_0$ .

By prescribing  $R_0$  which is the length between the center of the cone and the freestream surfaces. The free stream trailing edge is tailored respectively to equation (2).

$$X = R_0 + AY^2 \quad (2)$$

After the upper part of the base plane is formed, all points in the plane are pushed to the leading edge along to the freestream direction and intersect with the shock from the cone. The freestream surface is crafted by combining all

streamlines together. Finally, the compression surface is created by the description of the stream surface in the shock layer, where each point of the leading edge is projected back to the base plane to form a surface. In total, a cone-derived waverider contains three design variables:  $R_0$ ,  $\delta$  and  $\emptyset$ . The range of the design variables are defined as:  $30 \leq \emptyset \leq 70$ ,  $5 \leq \delta \leq 20$ ,  $0.2 \leq R_0 \leq 0.9$ .

## 2.2 Numerical Simulation

We use the Tohoku University Aerodynamic Simulation code (TAS) code to perform the computational fluid dynamic simulation [8-10]. The TAS code is a three-dimensional finite volume that uses the unstructured mesh technology [11]. The governing equation used in the present simulation is the inviscid Euler equation that is computed by the cell-vertex finite-volume scheme. Numerical inviscid flux is computed using the approximate Riemann solver of Harten-Lax-van Leer-Einfeldt-Wada (HLLEW) [12-15]. The flow conditions used in the present study are shown in Table 1. The evaluation of aerodynamic forces  $C_L$ ,  $C_D$ ,  $C_M$  and  $C_p$  represented the trend of design variable  $R_0$ ,  $\delta$  and  $\emptyset$ .

Table 1

Mach number	1.5
Governing Equation	Inviscid Euler equation
Mesh	Unstructured
Flight altitude	18000m
Aircraft length	8m

## 2.3 Sonic Boom Estimation

To estimate the sonic boom strength, a near-field overpressure information is needed. The near-field overpressure is obtained from numerical simulation and measured at the vertical (downward) distance 0.7 of vehicle length. After that, the sonic boom analysis tools called XNoise developed by JAXA [16,17], which is based on the augmented Burgers equations, is used to calculate the far-field

overpressure generated by a waverider. The governing equations are described as follows:

$$\frac{\partial p}{\partial x} = \frac{\beta}{2\rho_0 c_0^3} \frac{\partial p^2}{\partial t} - \frac{1}{2A} \frac{\partial A}{\partial x} p + \frac{1}{2\rho_0 c_0} \frac{\partial(\rho_0 c_0)}{\partial x} p \quad (3)$$

$$+ \frac{\delta}{2c_0^3} \frac{\partial^2 p}{\partial t^2} + \sum_i \frac{(\Delta c)_i \tau_i}{c_0^2} \left(1 + \tau_i \frac{\partial}{\partial t}\right)^{-1} \frac{\partial^2 p}{\partial t^2}$$

Basically, Equation (3) consists of five components, that is, nonlinearity, geometrical spreading, atmospheric stratification, thermoviscous absorption, and Relaxation. The calculations are done separately and finally integrated to give the final outcome that represents the far-field overpressure.

## 3 Optimization

### 3.1 Sampling Plan

To begin the optimization procedure, initial sample points are required first to generate and construct the surrogate models. In this study, the Halton sequence technique is used to create the initial samples. Halton sequence generates sample points from that are typically well distributed than those of the full factorial design method; moreover, it is possible to generate space-filling sequential sampling points through this method. Fig. 2 shows the sampling set consisting of 27 sampling points generated by Halton sequences used in this paper.

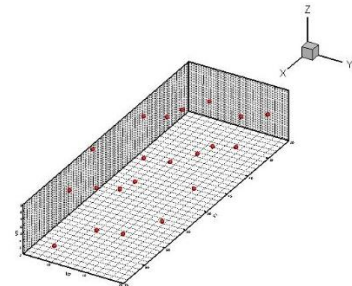


Fig. 2. A sampling plan based on Halton sequence with 27 sampling points.

### 3.2 Multi-Objective Optimization

The explanation of the whole optimization procedure is depicted in Fig. 3. First, the initial sample set is generated so as to create a space-filling sampling points. Next, the surrogate models are constructed by the OK method [18,19]. Here, the OK models provide both the function and error predictions which are important information for the execution of expected improvement strategy. Using these surrogate models, the Pareto-optimal solutions are then found by NSGA-II [20]. After that, some selected samples are evaluated using the numerical simulation and added to the experimental design. The process is then repeated until the computational budget exhausts. The goal is to minimize  $P_{fop}$ , maximize  $C_L$  and minimize absolute value of  $C_M$  under the constraint of 0.05 volumetric efficiency.

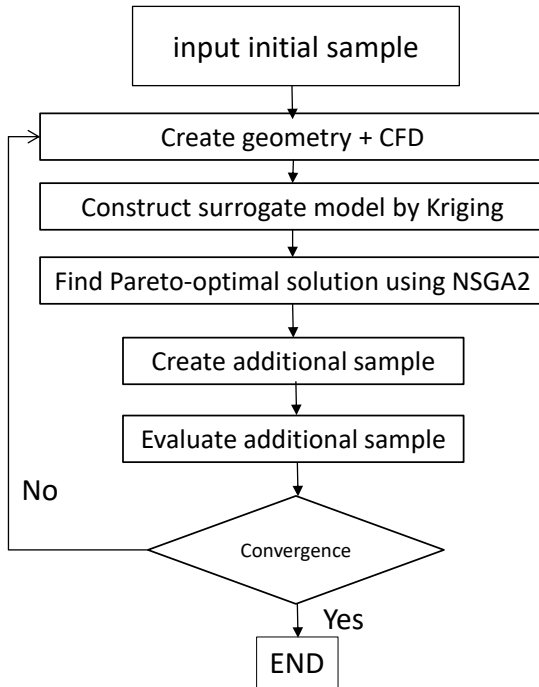


Fig. 3. The multi-objective optimization procedure of the present supersonic waverider design.

### 3.3 Sensitivity Analysis

Besides optimization, it is also important to extract useful insight and knowledge regarding the relationship between design variables and objective functions. Therefore, data mining of post-process optimization is essential to efficiently obtain the fruitful design knowledge. In this study, sensitivity analyses were conducted using a variance-based sensitivity analysis technique (i.e., Sobol indices). In general, sensitivity analysis is a method to evaluate the contributions of input parameters and their interactions to the outputs. The Sobol indices which is based on the idea of decomposing output variance to quantify the contribution of each input factor by increased dimension, where the total variance of the model is described in terms of the sum of the variances of the summands. Since Sobol' indices are traditionally evaluated by Monte Carlo simulation which makes them difficult to use when computationally expensive models are considered. In order to overcome this problem, this research uses polynomial chaos expansion surrogate model for sensitivity analysis (i.e., PCE-based Sobol indices) [21].

## 4 Result and Discussion

### 4.1 Parameter trend

The parametric study is observed based on 27 initial sample of full-factorial design. The range of design variables is determined from  $\emptyset=45,55,65$ ;  $\delta=5,10,15$ ;  $R_0=0.3,0.5,0.7$ .

#### 4.1.1 Lift-to-drag ratio

First, we present results of the parametric study. We observe that the L/D slightly increases when the value of  $\emptyset$  and  $\delta$  is increased and decreased, respectively. However,  $R_0$  gave a small number of uncertain change to L/D. Regarding the geometry shape, waveriders with high L/D tends to have slender body and thin wings; however, such designs are also less in volumetric efficiency which consider less practical for an additional integration of propulsion system such as engine. Figure 5



shows the geometry with the highest L/D, i.e., design WR6553 created from initial sample of parametric study.

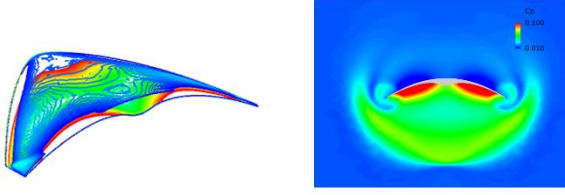


Fig. 4. The pressure distribution from the highest L/D waverider represented by the waverider model WR6553.

We can see that the waverider WR6553 possesses a slender wing shape with small volume. We infer that such design could potentially greatly reduce drag while increasing lift due to the fold-down of compression surface.

#### 4.1.2 Far-field overpressure

According to the result, the lowest  $P_{fop}$  (11.5 Pa) also comes from design parameters  $\phi = 65$ ;  $\delta = 5$ ;  $R_0 = 0.3Xs$  which is the same model as Fig.4, the highest L/D.

Here, the increase of  $\phi$  gives a low near-field overpressure which is proportionally to far-field overpressure. On the other hands, decreasing  $R_0$  can leads to slightly reduce  $P_{fop}$  as well. Decreasing  $\delta$  show the highest reduce of  $P_{fop}$ . Regarding to a vehicle shape in Fig.5, low-boom waverider (a) appear a small bump at the compression surface, but, the stronger overpressure waverider (b) shows smoother compression surface curve.

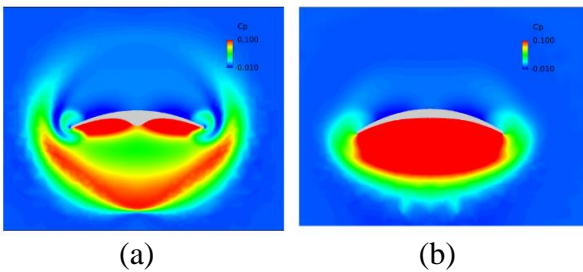


Fig. 5. Different of pressure distribution between a waverider with small bump at compression (a) surface and a waverider with smooth curve at compression surface (b).

## 4.2 Pareto-optimal solution

The results of optimized waverider in total 5 cycles (iteration), by adding 5 new samples in every cycle. Regarding to previous section, some of samples from parametric studied were brought to perform an optimization and to treat as the initial sample. The objective function  $C_L$  and  $P_{fop}$  showed some slightly improvement but still found some dominated solutions. Therefore, we added some additional samples until the fifth cycle of optimization procedure.

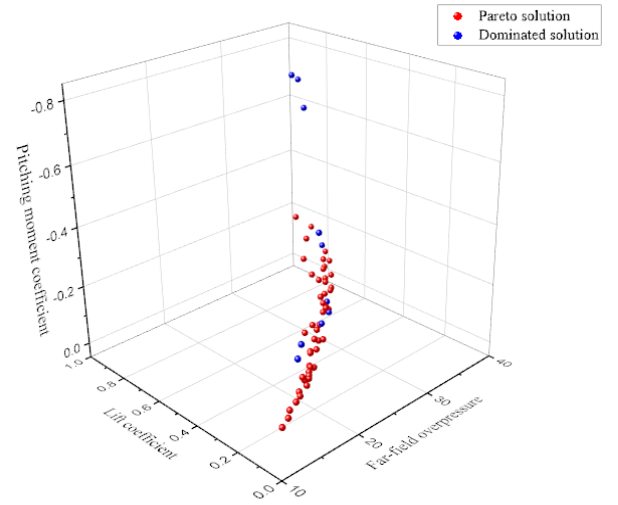


Fig. 6. Pareto-optimal solution of supersonic waveriders from the multi-objectives optimization ( $C_L$ ,  $C_M$  and  $P_{fop}$ ).

At the end, we obtained 25 additional samples (71 samples in total), the Pareto-optimal solutions were found in thin and narrow shape. In consequences, Pareto-optimal solutions cover most of initial samples as shown in Fig.6. Therefore, it is necessary to use a more complex set of waverider design variables that can provide high flexibility and degree-of-freedom of shape.

## 4.3 Analysis of PCE based Sobol indices

Since the purpose of this research is to investigate the variability of the model responses, the effect of design variable  $\phi$ ,  $\delta$  and  $R_0$  on  $C_L$ ,  $C_D$ ,  $C_M$  and  $P_{fop}$  are analyzed by using the PCE-based Sobol indices technique. The results are shown in Fig. 7 which contains the main effect of the variables and their interactions.

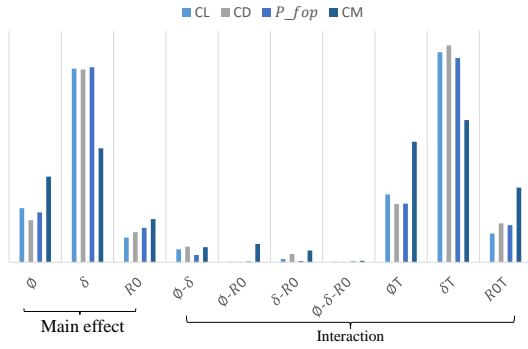


Fig. 7. PCE-based sensitivity analysis between design variables and objective function. The chart explains about main effect and interaction effect of each pair of variable.

Regarding the main effect, we observe that the variable  $\delta$  yields the highest impact to all outputs ( $C_L = 0.6690$ ,  $C_D = 0.6665$ ,  $C_M = 0.6743$  and  $P_{fop} = 0.6743$ ) where both  $\phi$  and  $R_0$  shows smaller impact. Among the interaction terms, the couple of  $\phi - \delta$  shows the highest impact to three outputs (i.e.,  $C_L = 0.0447$ ,  $C_D = 0.0538$ ,  $C_M = 0.0251$  and  $P_{fop} = 0.0521$ ); however,  $\phi - R_0$  yields the highest sensitivity to  $C_M$ . For the total interaction,  $\delta$  is the most dominant variable followed by  $\phi$  and  $R_0$ . Since  $\delta$  is the most impactful variable, it means that the thickness of the supersonic waverider is the most important factor, followed by the concave shape of the lower surface that is related to  $\phi$ . Basically our investigation shows that the concept of low-boom supersonic waverider is possible to achieve.

## 5 Conclusion

This research introduces the cone-derived waverider method for dealing with common supersonic aircraft problems of reducing sonic boom while maximizing aerodynamic performance. First, a parametric study was performed via numerical simulation and three design variables (i.e.,  $R_0$ ,  $\delta$  and  $\phi$ ) that describe the waverider shape. Results show that all three design parameters show significant impact to sonic boom reduction in different ways. Here, a small value of cone angle yields a dominant effect in terms of minimizing sonic boom strength and maximizing lift-to-drag ratio.

Next, we perform multi-objective optimization using the same design variable as parametric study and lift coefficient, pitching moment coefficient and far-field overpressure as objectives function. The surrogate-models based on Kriging and NSGA2 are used as the optimizer. Lastly, we performed sensitivity analysis using PCE-based Sobol technique. It is found that the most dominant variable is cone angle and dihedral angle respectively in terms of both the main effect and interactions.

For future work, we are planning to investigate more complex shapes of waverider incorporated into multi-objective optimization study. Such study is important to further analyze the potentials and pitfalls of waverider design for the realization of supersonic aircraft.

## References

- [1] K. Kusunose, K. Matsushima, Y. Goto, H. Yamashita, M. Yonezawa, D. Maruyama, and T. Nakano. A Fundamental Study for the Development of Boomless Supersonic Transport Aircraft. *Proc 44th Aerospace Sciences Meeting and Exhibit, Aerospace Sciences Meetings*, 2006.
- [2] Nonweiler T.R.F. Delta Wings of Shape Amenable to Exact Shock Wave Theory. *Journal of the Royal Aeronautical Society*, Vol. 67, pp 39, 1963.
- [3] J.D. Anderson Jr. *Modern Compressible Flow (with Historical Perspective)*. 3<sup>rd</sup> edition, McGraw-Hill, 2003.
- [4] S. Corda, J.D. Anderson Jr. Viscous Optimized Hypersonic Waveriders Design from Axisymmetric Flow Fields. *Proc 26th Aerospace Sciences Meeting and Exhibit, Aerospace Sciences Meetings*, 1988.
- [5] Rasmussen, M.L., He, X. Analysis of Cone-Derived Waverider by Hypersonic Small-Disturbance Theory. *Proc The First International Hypersonic Waverider Symposium*, 1990.
- [6] Rolim, T.C., Toro, P.G.P., Minucci, M.A.S, Oliveira, A.C., Follador, R.C. Experimental Results of a Mach 10 Conical-flow Derived Waverider to 14-X Hypersonic Aerospace Vehicle. *Journal of Aerospace Technology and Management*, Vol.3, pp 127-136, 2011.
- [7] S.C. Lin and M.C. Shen, B.J. Tsai. Establishment of Approximate Equations for Waverider with Multi-Directional-Curvature, *Proc 33rd Aerospace Sciences Meeting and Exhibit, Aerospace Sciences Meetings*, 1995.

- [8] Nakahashi, K., Ito, Y. and Togashi, F. Some Challenge of Realistic Flow Simulations by Unstructured Grid CFD, *International Journal for Numerical Methods in Fluids*, Vol. 43, No. 6-7, pp 769-783, 2003.
- [9] Obayashi, S. and Guruswamy G. P. Convergence Acceleration of a Navier-Stokes Solver for Efficient Static Aeroelastic Computations. *AIAA Journal*, Vol.33, No.6, pp 1134-1141, 1994.
- [10] Roe, P. L. Approximate Riemann Solvers, Parameter Vectors, and Difference Schemes. *Journal of Computational Physics*. Vol.43, No.2, pp 357-372, 1981.
- [11] Sharov, D. and Nakahashi, K. Reordering of Hybrid Unstructured Grids for Lower-Upper Symmetric Gauss-Seidel Computations. *AIAA Journal*, Vol. 36, No. 3, pp 484-486, 1998.
- [12] Jameson, A. and Turkel, E. Implicit Schemes and LU decomposition. *Mathematics of Computation*. Vol.37, No. 156, pp 385-397, 1981.
- [13] Sharov, D. and Nakahashi, K. Hybrid Prismatic/Tetrahedral Grid Generation for Viscous Flow Applications. *AIAA Journal*. Vol. 36, pp 157-162, 1998.
- [14] Ito, Y. and Nakahashi, K. Direct Surface Triangulation Using Stereolithography (STL) Data. *AIAA Journal*, Vol. 40, No. 3, pp 490-496, 2000.
- [15] Sharov, D. and Nakahashi, K. Hybrid Prismatic / Tetrahedral Grid Generation for Viscous Flow Applications. *AIAA Journal*. Vol. 34, No.2, pp 291-298, 1996.
- [16] Yamamoto, M., Hashimoto, A., Takahashi, T., Kamakura, T. and Sakai, T. Numerical Simulation for Sonic Boom Propagation through an Inhomogeneous Atmosphere with Winds. *AIP Journal*. Vol. 1474, pp.339-342, 2012.
- [17] H. Ishikawa, Y. Makino, T. Ito and F. Kuroda. Sonic Boom Prediction Using Multi-Block Structured Grids CFD Code Considering Jet-On Effects. *Proc 27th AIAA Applied Aerodynamics Conference*. Vol. 3508, 2009.
- [18] Alexander F., Adras S. Andy K. *Engineering Design via Surrogate Modelling*. John Wiley & Sons, 2008.
- [19] Deb, K. *Multi-Objective Optimization Using Evolutionary Algorithms*. John Wiley & Sons, 2001.
- [20] Deb, K., Pratap, A., Agarwal, S., and Meyarivan, T. A Fast and Elitist Multiobjective Genetic Algorithm: NSGA-II. *IEEE Transactions on Evolutionary Computation*, Vol. 6, No. 2, pp. 182-197, 2002.
- [21] S. Marelli, C. Lamas, B. Sudret. *UQLAB User Manual – Sensitivity Analysis*. ETHzurich, 2015.

## Contact Author Email Address

boonjaipetch.potsawat.s4@dc.tohoku.ac.jp

## Copyright Statement

The authors confirm that they, and/or their company or organization, hold copyright on all of the original material included in this paper. The authors also confirm that they have obtained permission, from the copyright holder of any third party material included in this paper, to publish it as part of their paper. The authors confirm that they give permission, or have obtained permission from the copyright holder of this paper, for the publication and distribution of this paper as part of the ICAS proceedings or as individual off-prints from the proceedings.